RESEARCH ARTICLE

Combination of olfactory ensheathing cells and human umbilical cord mesenchymal stem cell-derived exosomes promotes sciatic nerve regeneration

Yang Zhang[1, #], Wen-Tao Wang[2, #], Chun-Rong Gong[3, #], Chao Li[4, *], Mei Shi[1, *]

1 Department of Radiation Oncology, Xijing Hospital, Air Force Medical University, Xi'an, Shaanxi Province, China
2 Department of Orthopedics, Changhai Hospital, Naval Medical University, Shanghai, China
3 Rehabilitation Center, North District Hospital of the People's Hospital of Lin Yi City, Linyi, Shandong Province, China
4 Department of Orthopedics, The Eighth Medical Center of Chinese PLA general Hospital, Beijing, China

Funding: *This work was supported by grants from the National Natural Science Foundation of China, No. 81872699 (to MS), Key project of Shaanxi Province, China, No. 2017ZDXM-SF-043 (to MS), and the Military Medical Science and Technology Youth Development Program, China, No. 19QNP061 (to CL).*

Graphical Abstract

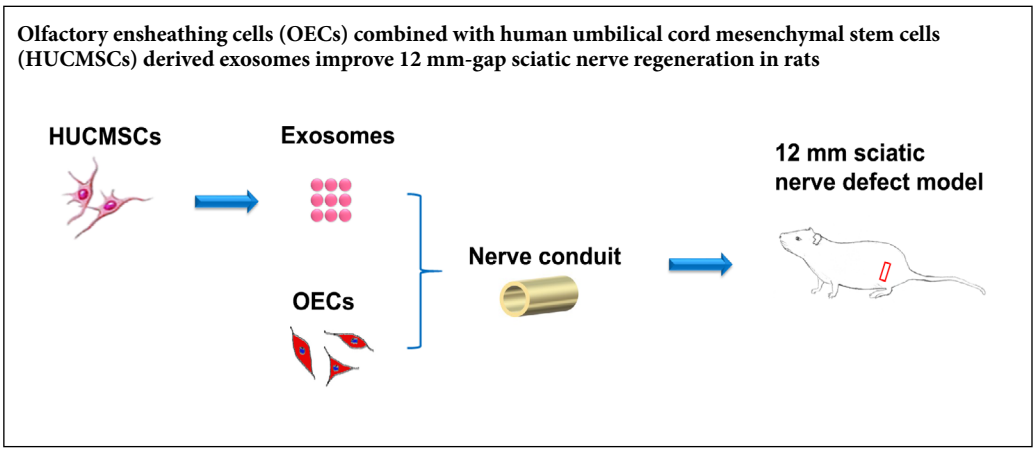

Correspondence to:
Mei Shi, PhD, mshi82@hotmail.com;
Chao Li, PhD, Chnmedli@126.com.

#These authors contribute equally to this work.

orcid:
0000-0002-4937-405X
(Mei Shi)
0000-0001-7135-2503
(Chao Li)

doi: *10.4103/1673-5374.280330*

Received: *October 15, 2019*
Peer review started: *October 24, 2019*
Accepted: *December 31, 2019*
Published online: *April 3, 2020*

Abstract

Olfactory ensheathing cells (OECs) are promising seed cells for nerve regeneration. However, their application is limited by the hypoxic environment usually present at the site of injury. Exosomes derived from human umbilical cord mesenchymal stem cells have the potential to regulate the pathological processes that occur in response to hypoxia. The ability of OECs to migrate is unknown, especially in hypoxic conditions, and the effect of OECs combined with exosomes on peripheral nerve repair is not clear. Better understanding of these issues will enable the potential of OECs for the treatment of nerve injury to be addressed. In this study, OECs were acquired from the olfactory bulb of Sprague Dawley rats. Human umbilical cord mesenchymal stem cell-derived exosomes (0–400 μg/mL) were cultured with OECs for 12–48 hours. After culture with 400 μg/mL exosomes for 24 hours, the viability and proliferation of OECs were significantly increased. We observed changes to OECs subjected to hypoxia for 24 hours and treatment with exosomes. Exosomes significantly promoted the survival and migration of OECs in hypoxic conditions, and effectively increased brain-derived neurotrophic factor gene expression, protein levels and secretion. Finally, using a 12 mm left sciatic nerve defect rat model, we confirmed that OECs and exosomes can synergistically promote motor and sensory function of the injured sciatic nerve. These findings show that application of OECs and exosomes can promote nerve regeneration and functional recovery. This study was approved by the Institutional Ethical Committee of the Air Force Medical University, China (approval No. IACUC-20181004) on October 7, 2018; and collection and use of human umbilical cord specimens was approved by the Ethics Committee of the Linyi People's Hospital, China (approval No. 30054) on May 20, 2019.

Key Words: *brain-derived neurotrophic factor; cell migration; cell viability; functional recovery; hypoxia; nerve regeneration; sciatic functional index; sciatic nerve injury*

Chinese Library Classification No. *R456; R741; R363*

Introduction

Olfactory ensheathing cells (OECs), a type of glial cell, are specifically located in the olfactory system. Based on their capability to promote axon extension, express various neurotrophic factors, and modulate the immune response, OECs have been applied to the treatment of peripheral nerve defect, spinal cord injury, Parkinson's disease, and glioma (Gomes et al., 2018; Liu et al., 2018; Carvalho et al., 2019; Zhang et al., 2019a). However, a long-term hypoxic micro-milieu at the site of injury or disease greatly attenuates the therapeutic use of OECs, especially because their migratory ability is restricted, which limits their effective use for

the treatment of peripheral nerve injury (Zhu et al., 2014; Wang et al., 2016). Therefore, it is necessary to find a strategy to enhance the migration efficiency of OECs in hypoxic conditions to improve the therapeutic efficacy of OECs in nerve regeneration.

Human umbilical cord mesenchymal stem cells (HUCMSCs) can improve neonatal memory, promote traumatic brain injury repair, and prevent fibrosis pathology in a hypoxic microenvironment, indicating that HUCMSCs are capable of ameliorating hypoxic conditions (Shi et al., 2016; Zhang et al., 2017; Zhu et al., 2019a). However, limitations of HUCMSCs, include phenotypic changes during cell proliferation, a long incubation time, and decreased survival of transplanted cells (Wang et al., 2018). Therefore, new strategies have been introduced to eliminate these disadvantages. Recent studies have reported that exosomes from HUCMSCs are capable of alleviating acute liver failure, enhancing porcine islet resistance under hypoxia, and reducing neuroinflammation in perinatal brain injury (Nie et al., 2018; Jiang et al., 2019; Thomi et al., 2019). Exosomes are artefactual cup-shaped membrane vesicles 40–150 nm in diameter that are secreted from live cells. They act as communicators in cell-to-cell interaction and exert an important influence on physiological and pathological processes (Zhang et al., 2019b). However, the effect of HUCMSC exosomes on the migratory ability of OECs is unknown, especially in hypoxic environments, and the synergistic effect of OECs and exosomes on peripheral nerve injury repair is controversial. Therefore, illumination of these issues will enable the biological effects of OECs on nerve injury treatment to be resolved.

In this study, we first isolated exosomes from HUCMSCs and characterized their features. Then, the viability and migration of OECs with exosomes under hypoxic conditions were tested. Most importantly, the mechanism by which exosomes enhance OECs was analyzed. Finally, the promotion of axon outgrowth and regeneration, and functional recovery by OECs and exosomes was investigated.

Materials and Methods

Isolation and cultivation of OECs

OECs were acquired from the olfactory bulb of male Sprague Dawley (SD) rats (aged 28–35 days, weight 100–150 g, specific pathogen free) obtained from the Experimental Animal Center of the Air Force Medical University, China [Xi'an, Shaanxi Province, China; animal license No. SCXK (Army) 2012-0007]. All procedures were approved by the Institutional Ethical Committee of the Air Force Medical University (approval No. IACUC-20181004) on October 7, 2018. The isolation and purification procedures were based on a previously described protocol (Zhu et al., 2014). Briefly, after deep isoflurane anesthesia, rats were killed by decapitation and the olfactory bulbs were harvested from the opened skull. One caudal third of the bulb was removed and the white matter was discarded. The tissue was gently minced and then incubated in a sterile solution containing 0.75 mg/mL collagenase A (Cat# 10103578001; Roche, Mannheim, Germany), 0.75 mg/mL collagenase D (Cat# 11088858001; Roche), and 12 U/mL papain (Cat# 10108014001; Roche) with cysteine for 25 minutes (37°C, 5% CO_2). The tissue suspension was centrifuged at 350 × *g* for 8 minutes, and the tissue precipitate was re-suspended in Dulbecco's modified Eagle's medium/nutrient mixture F-12 (DMEM/F12; Cat# 11320033; Gibco, Burlington Ontario, Canada) containing 20% fetal bovine serum (FBS; Cat# 10099141; Gibco, Melbourne, Australia) for termination of digestion. After centrifugation, the tissue pellet was re-suspended in DMEM/F12 with 10% FBS and incubated for 18 hours to remove non-adherent cells. The cells were re-suspended in DMEM/F12 with 10% FBS and incubated in a CO_2 atmosphere at 37°C. The medium was exchanged every 2–3 days. The purity of the OECs was confirmed by the average ratio of glial fibrillary acidic protein (GFAP; 1:200; Cat# ab7260; rabbit polyclonal; Abcam, Cambridge, MA, USA) and nerve growth factor receptor p75 (NGFRp75; 1:200; Cat# ab3125; mouse monoclonal, Abcam) double-immunopositive cells to 4′,6-diamidino-2-phenylindole (DAPI; 10 μg/mL; Cat# MBD0015-1ML; Sigma-Aldrich, St. Louis, MO, USA)-labeled cells. The primary GFAP and NGFRp75 antibodies were incubated at 4°C for 12 hours. Then, they were stained for 60 minutes at room temperature with Alexa 488 goat anti-rabbit IgG (1:250; Cat# ab150077; Abcam) and Alexa 594 goat anti-mouse IgG (1:250; Cat# ab150116; Abcam).

Identification of HUCMSCs

Human umbilical cords were collected from two full-term pregnant women after cesarean delivery with prior written informed consent from the women and approval authorized by the Ethics Committee of the Linyi People's Hospital, China (approval No. 30054) on May 20, 2019. The isolation and cultivation methods were based on a previously described protocol (Wang et al., 2018). In detail, the tissues were washed with 75% ethanol and later with DMEM/F12 complete medium to remove excess blood. Then, the tissues were divided into small tissue blocks (2.0 mm^2), placed in a 10-mm culture plate and incubated with complete medium at 37°C in 5% CO_2. When the cells were about 80% confluent, they were trypsinized for subculture. HUCMSC-specific markers were evaluated by flow cytometry. Multi-cell differentiation was conducted for osteogenesis, adipogenesis, and chondrogenesis (Wang et al., 2018). The HUCMSCs used in this study were passaged no more than five times. Images of cells were obtained using a light microscope (Olympus Corporation, Tokyo, Japan).

Isolation and characterization of exosomes

When HUCMSCs were approximately 80–85% confluent, incubation was continued in cell culture medium without FBS for 72 hours. Culture medium (40 mL/tube) was then centrifuged at 300 × *g* for 15 minutes and then at 2000 × *g* for 30 minutes at 4°C to remove debris and dead cells. The supernatant was then ultra-centrifuged at 100,000 × *g* for 150 minutes at 4°C. The final pellet, which contained exosomes, was re-suspended in 500 μL phosphate buffered saline (PBS). The concentration of exosomes was determined using a bicinchoninic acid method (Xu et al., 2020) and evaluated by transmission electron microscopy (FEI, Hillsboro, OR, USA) and Zetasizer Nano ZS molecular size analysis (Malvern Instruments, Worcestershire, UK). Specific markers of HUSMSCs exosomes, including heat shock protein 70 (Cat# ab2787; mouse; Abcam), CD9 (Cat# ab2215; mouse; Abcam), and CD63 (Cat No. ab59479; mouse; Abcam), were analyzed by western blot assays. In detail, the protein extracts (10 μg per sample) were boiled for 5 minutes, electrophoretically sep-

arated in 15% sodium dodecyl sulfate-polyacrylamide gels, and transferred to nitrocellulose membranes. Membranes were blocked in 5% skimmed milk in TBTS buffer and then incubated with mouse anti-heat shock protein 70 (1:1000), anti-CD9 (1:1000), and anti-CD63 (1:1000) antibodies at 4°C overnight. The membranes were washed gently three times with TBTS and then immersed in HRP-conjugated goat anti-mouse IgG (1:500; Cat# ab205719; Abcam) solution for 60 minutes at room temperature. The membranes were then washed three times with PBS, immersed in an electroluminescence reagent (Pierce ECL™ Plus substrate, Cat# 32132, 1:1000, Thermo Scientific, Rockford, IL, USA) and photographed using a GS 800 Densitometer Scanner (GMI, Ramsey, MN, USA).

Cell Counting Kit 8 (CCK-8) assay

The viability of OECs in the presence of different concentrations (0, 50, 100, 200, and 400 μg/mL) of exosomes was quantified by CCK-8 assays (Cat# CK04-01; Dojindo, Kumamoto, Japan). To standardize the cell quantity, the same number of OECs (about 1×10^6 cells/well) was incubated in a 6-well plate for each group. The OECs were then incubated with different concentrations of exosomes. At 12, 24 and 48 hours, OECs were rinsed three times with PBS and then digested with a 0.05% trypsin solution, washed, re-suspended in DMEM/F12 and cultured in a 96-well plate (100 μL/well). Ten microliters of CCK-8 solution were dropped gently into each well and incubated for 4 hours. The absorbance at 492 nm was calculated using a multi-mode reader (CLARIOstar plus, BMG LABTECH, Cary, NC, USA). Cells were cultured with PBS as a negative control.

5-Ethynyl-2′-deoxyuridine assays

The proliferation of OECs in the presence of different concentrations of exosomes was analyzed by 5-ethynyl-2′-deoxyuridine (EdU) assays (Cat# C10310; RiboBio; Guangzhou, China). To standardize the cell quantity, the same number of OECs (about 1×10^5 cells/well) was incubated in a 24-well plate for each group. Twenty-four hours after exosome administration, EdU was added and the OECs were fixed 4 hours later. The EdU solution was then removed and the OECs were gently rinsed with PBS three times. Finally, DAPI was used to stain the cell nuclei, and the EdU-labeling index was determined by comparing the number of EdU-stained nuclei and DAPI-stained nuclei. Cells were cultured with PBS as a negative control.

Immunostaining of OECs and exosomes under hypoxia

After co-cultivation with PKH-26-labeled (Cat# MIDI26-1KT; Sigma-Aldrich) exosomes, OECs were cultured in a humidified hypoxic incubator (OECs + hypoxia + Exos group; 37°C, 0.5% O_2, 5% CO_2) for 24 hours. Cells were then immunofluorescence stained. All procedures were performed in a dark room. In detail, cells were fixed with 4% paraformaldehyde for 15 minutes, incubated with 0.2% Triton X-100 solution for 10 minutes, and then treated with 10% goat serum blocking solution for 30 minutes at room temperature. Cells were then incubated with an anti-GFAP (1:200; rabbit polyclonal; Abcam) primary antibody overnight at 4°C. The following day, DAPI was used to stain cell nuclei. Quantification of OECs was then performed. OECs with exosomes (OECs + Exos group) or without exosomes (OECs group) in normal oxygen conditions were also quantified. OECs without exosomes in hypoxic conditions (OECs + hypoxia group) were used as a control group.

Cell migration assay

The migration of OECs was evaluated using a Transwell chamber (Cat# MCEP24H48; Millipore, St. Louis, MO, USA). One hundred microliters of the OECs (1×10^5 cells/mL) were placed in the top chamber. After incubation for 12, 24 or 48 hours under hypoxic conditions, cells on the top chamber membrane were gently removed and cells adhered on the lower chamber membrane were stained with hematoxylin-eosin. The cells were then observed under a light microscope (Olympus).

Gene-expression assay

OECs (1×10^6 cells/well) were cultured for 24 hours and were then incubated for a further 24 hours in hypoxic conditions. The OECs were then homogenized in Trizol reagent (Cat# 93289; Sigma-Aldrich) and total RNA was harvested. Brain-derived neurotrophic factor (*Bdnf*) mRNA was analyzed by quantitative real-time polymerase chain reaction (qRT-PCR). Primer sequences for *Bdnf* and *β-actin* were: *Bdnf*, 5′-AGT GCC GAA CTA CCC AGT CGT A-3′ (forward) and 5′-CTT ATG AAT CGC CAG CCA ATT C-3′ (reverse); *β-actin*, 5′-GAG ACC TTC AAC ACC CCA G-3′ (forward) and 5′-GAG ACC TTC AAC ACC CCA G-3′ (reverse) (Zhao et al., 2011; de Farias et al., 2012). The PCR was performed as follows: denaturation at 95°C for 40 seconds; primer annealing at 60°C for 35 seconds; elongation at 65°C for 40 seconds. The data were analyzed using the $2^{-\Delta\Delta Ct}$ method.

Western blotting

OECs (1×10^6 cells/well) were cultured for 24 hours, incubated in hypoxic conditions for another 24 hours, and then lysed with lysis buffer for protein extraction. Then protein extracts (30 μg per sample) were boiled for 5 minutes, electrophoretically separated on 15% sodium dodecyl sulfate-polyacrylamide gels, and then transferred to nitrocellulose membranes. Membranes were then blocked with 5% skimmed milk in TBTS buffer and then incubated with a rabbit anti-BDNF (1:1000; Cat# ab108319; Abcam) monoclonal antibody at 4°C overnight. Membranes were washed gently three times with TBTS and then immersed in HRP-conjugated goat anti-rabbit IgG (1:500; Cat# ab205718; Abcam) solution for 60 minutes. Membranes were washed three times with PBS, immersed in an electroluminescence reagent and photographed using a GS 800 Densitometer Scanner (GMI, Ramsey, MN, USA).

Enzyme-linked immunosorbent assay

OECs (1×10^6 cells/well) were cultured for 24 hours and then incubated in hypoxic conditions for another 24 hours. OECs were then counted and the amount of BDNF secreted into the culture medium determined. The assay was performed by using a commercial enzyme-linked immunosorbent assay (ELISA) kit (Cat# ABIN5609809; Antibodies Online, Limerick, PA, USA) and a microELISA reader (Multiscan MK3; Thermo Scientific, Waltham, MA, USA) according to the manufacturers' instructions. The quantity of

BDNF secreted by OECs was normalized to the cell number.

Animal surgical procedures

All animal experiments were conducted with the ethical approval of the Institutional Ethical Committee of the Air Force Medical University. Chitosan-collagen conduits were fabricated as previously described (Zhu et al., 2014) and used to carry cells. Male SD rats (aged 42–56 days, weight 220–250 g, specific pathogen free) from the Experimental Animal Center of the Air Force Medical University were randomly divided into five groups (n = 10 per group) to evaluate sciatic nerve regeneration *in vivo*. The groups included autograft, conduits (non-filled), OECs [conduits filled with 10 μL OECs (5×10^5)], Exos [conduits filled with 10 μL exosomes (400 μg/mL)], and OECs + Exos groups [conduits filled with 10 μL OECs (5×10^5) and exosomes (400 μg/mL)]. All animals were anesthetized with 3.5% isoflurane gas. A 12 mm excision was made in the left sciatic nerve as described previously (Wang et al., 2013). In the autograft group, the severed sciatic nerve was turned through 180° and sutured back into the sciatic nerve. In the other four groups, the conduits with different contents were implanted and both the proximal and distal ends of the sciatic nerve were sutured using 10-0 Prolene sutures with a depth of 1 mm into the conduits.

Immunohistochemistry

Twelve weeks post-surgery, the middle portions of the harvested conduits with regenerative nerves were longitudinally sectioned. The sections were incubated with anti-S-100 (for Schwann cells; 1:250; Cat# ab183979; rabbit monoclonal; Abcam), and anti-neurofilament 200 (for regenerated axons; 1:250; Cat# ab82259; mouse monoclonal; Abcam). at 4°C for 12 hours and then with Alexa 594 goat anti-rabbit IgG (1:250; Cat# ab150080; Abcam) and Alexa 488 goat anti-mouse IgG (1:250; Cat# ab150117; Abcam) secondary antibodies 60 minutes. Sections were observed using a fluorescence microscope (DM6000, Leica, Buffalo Grove, IL, USA).

Functional assessment

At 4, 8, and 12 weeks post-surgery, evaluation of animals' motor function was assessed using the walking track test as previously described (Hare et al., 1992). The hind paws of rats were daubed with nontoxic dye and footprints produced by the walking test were photographed. The sciatic functional index (SFI) was analyzed with the following parameters: (1) toe spread (TS), the distance between the first and fifth toes; (2) intermediary toe spread (IT), the distance between the second and the fourth toes; (3) print length (PL), the distance between the heel and the top of the third toe. The SFI formula was: SFI = –38.3 × (EPL – NPL)/NPL + 13.3 × (EIT – NIT)/NIT + 109.5 × (ETS – NTS)/NTS – 8.8. N is the non-surgical foot, and E is the experimental foot. A score of –100 represents total dysfunction.

Sensory functional recovery of the animals was conducted after the SFI experiment using the plantar assay according to previously described protocols (Song et al., 2017; Montagne-Clavel and Oliveras, 1996). The left hind paw of the animal was stimulated using radiant heat (about 46.5°C). The latency time until a hind paw lick or shake/jump was recorded. The stimulation was conducted only once at each time point to prevent sensitivity and was suspended to avoid heat injury if the heat time was up to 30 seconds. The normal group was non-injured rats and provided the latency base line.

All functional assessments were conducted before surgery to determine the baseline data.

Electrophysiological evaluation

Electrophysiological analysis was conducted on rats before the histological experiments at 4, 8, and 12 weeks post-surgery. Rats were anesthetized and the operated sciatic nerve was gently exposed. A bipolar stimulatory electrode (BL-420F; Taimeng Science and Technology Co., Ltd., Chengdu, China) was placed beneath the sciatic nerve at a distance of 10 mm from the nerve graft. The recording electrode was located within the gastrocnemius muscle. The nerve conduction velocity and latency were recorded for quantitative analysis as previously described (Suzuki et al., 1999).

Statistical analysis

All data are presented as the mean ± standard error of mean or standard deviation. Bonferroni's test was used to analyze the effects of time and treatments for paired comparisons. One-way analysis of variance was conducted to evaluate mean values using SPSS 20.0 software (IBM, Armonk, NY, USA). $P < 0.05$ represents statistical significance.

Results

Identification of OECs

Figure 1 shows OECs with a spindle-shaped morphology. The purity of OECs was analyzed by double-immunofluorescence staining with GFAP (green) and P75 (red). The numbers of GFAP and P75 double-positive cells and DAPI-dyed cells were compared. The purity of OECs was more than 96% for the following experiments.

Characterization of HUCMSCs and exosomes

HUCMSC surface markers were characterized by flow cytometry. The profiles of CD44, CD49, CD73, CD90, CD105, and CD146, and human leukocyte antigen-A, B, and C were positive, with a high level of expression ≥ 97%. The profiles of CD14, CD31, CD34, and CD45, and human leukocyte antigen-DR were negative, with a low level of expression ≤ 1% (**Figure 2A**). HUCMSCs were observed under a light microscope (**Figure 2B**). The multiple differentiation capacities of HUCMSCs were confirmed for osteogenesis, adipogenesis, and chondrogenesis (**Figure 2C–E**). These characteristics determined that the cells were HUCMSCs. The morphological appearance of exosomes from HUCMSCs was then performed by transmission electron microscopy. The typical artefactual cup-shaped membrane of exosomes was observed (**Figure 2F**). Their dimensions ranged from 30 to 160 nm, and their average diameter was 75.28 nm (**Figure 2G**). In addition, the specific exosomal markers, heat shock protein 70, CD9, and CD63, were detected by western blot assays (**Figure 2H**).

Exosomes from HUCMSCs increase the viability of OECs

Different concentrations of exosomes from HUCMSCs were applied to OECs. The CCK-8 test (**Figure 2I**) showed that an exosome concentration was 400 μg/mL produced the highest absorbance at 492 nm after incubation for 12, 24, and 48

hours. Meanwhile, the EdU-labeling index (**Figure 2J**) showed that the proliferation rate of OECs with 400 μg/mL exosomes was significantly higher after incubation for 24 hours compared with other exosome concentrations. Therefore, an exosome concentration of 400 μg/mL was used in subsequent experiments.

HUCMSC exosomes increase the number of OECs under hypoxia

To track exosomes with OECs, exosomes were stained with PKH26 before combining with OECs. Under hypoxic conditions, the number of OECs was significantly lower compared with that in normal conditions (**Figure 3A–H** and **Q**). With the administration of exosomes, the number of OECs was 1.76- and 4.62-fold higher compared with that in normal and hypoxic conditions, respectively (**Figure 3A–L** and **Q**). Intriguingly, exosomes were able to rescue the negative effect of hypoxia on OECs, with a 3.83-fold higher number compared with that in hypoxic conditions (**Figure 3E–H** and **M–Q**). Moreover, the number of OECs in the OECs + hypoxia + Exos group was 1.47-fold higher than that in the OECs group (**Figure 3A–D** and **M–P**).

HUCMSC exosomes enhance the migration of OECs in hypoxic conditions by promoting BDNF

The migration capability of OECs was analyzed by calculating the number of OECs that migrated through Transwell chambers. As shown in **Figure 4**, when incubated in hypoxic conditions without exosomes, the numbers of migrated OECs were 0.35-, 0.35-, and 0.38-fold lower than those under normal conditions at 12, 24, and 48 hours, respectively (**Figure 4B**, **C**, and **F**). Meanwhile, the number of migrated OECs was significantly increased in the OECs + Exos group in comparison with other groups (**Figure 4D** and **F**). Conversely, migrated OECs were significantly increased by exosomes under hypoxic conditions, indicating that exosomes were able to enhance the migration ability of OECs under hypoxia (**Figure 4E** and **F**). Moreover, the gene expression, protein level and secretion of BDNF were evaluated by qRT-PCR, western blotting, and ELISA, respectively, and the results showed that exosome treatment significantly promoted the gene expression, protein level and secretion of BDNF in OECs under hypoxic conditions (**Figure 4G–J**), indicating that the increased migration of OECs by exosomes under hypoxic conditions was partly attributed to enhanced BDNF expression and secretion.

OECs and exosomes synergistically promote nerve regeneration

The morphology of regenerated nerves was observed using double neurofilament 200/S-100 immunofluorescence staining of the middle sections of the harvested tissues. **Figure 5M–O** shows that at 12 weeks post-surgery the regenerated axons and migrated Schwann cells were evenly distributed in the OECs + Exos group, similar to those in the autograft group (**Figure 5A–C**). The regenerative nerve appearance was better in the OECs + Exos group and the autograft group compared with that in the conduits (**Figure 5D–F**), OECs (**Figure 5G–I**), and Exos groups (**Figure 5J–L**).

OECs and exosomes synergistically improve functional recovery of injured sciatic nerve

Motor and sensory functional recovery was observed in all groups (**Figure 6A–C**) at 4, 8, and 12 weeks post-operation. Better functional motor recovery with higher SFI index and higher nerve conduction velocity was found in the OECs + Exos group compared with that in the conduits, OECs, and Exos groups ($P < 0.05$; **Figure 6A** and **B**). Moreover, animals in the OECs + Exos group showed better sensory functional recovery with faster latency compared with that in the conduits, OECs, and Exos groups ($P < 0.05$; **Figure 6C**).

Discussion

In this study, we demonstrated the effect of HUCMSC exosomes on the viability of OECs and we then evaluated the improvement that exosomes make on OEC migration under hypoxic conditions. In addition, we show that BDNF was partly responsible for the promotion of OEC migration in hypoxic conditions. The combination of OECs and exosomes improved nerve regeneration and functional recovery. These findings highlight the potential for exosome-modified OECs in peripheral nerve injury regeneration.

Long-term low oxygen levels in sites of injury are a major hindrance in cell transplantation and tissue repair, especially for sciatic nerve defects. Wang et al. (2013) and Zhu et al. (2014) reported low oxygen levels within nerve grafts that significantly limited nerve regeneration and functional recovery after nerve injury; however, increasing oxygen concentration in the sciatic nerve long-gap (> 10 mm) model using oxygen carrier biomaterial increased viability of the transplanted cells and promoted nerve regeneration *in vivo*. Therefore, we chose the 12 mm sciatic nerve defect in rats to create long-term hypoxic conditions *in vivo*.

OECs are a specific class of glial cell in the olfactory system with multiple properties, such as promoting axonal growth, and expressing neurotrophic factors (Beecher et al., 2018; Gu et al., 2019). Recent studies have shown that OEC transplantation is a promising strategy for treating peripheral nerve injury (Zhang et al., 2019a), spinal cord injury (Gomes et al., 2018), brain disease (Liu et al., 2018), and glioma (Carvalho et al., 2019), in part because of the enhanced migratory potential of OECs (Riggio et al., 2013). In these complex environments, OECs have to migrate from transplanted sites to injured sites, and must interact with various surrounding cells and factors. To enhance the migratory capability of OECs and to overcome the effect of hypoxia on OECs, new strategies are being developed, including the application of exosomes.

In recent years, exosomes derived from HUCMSCs have been shown to modulate several diseases and injury processes, especially in hypoxic conditions (Nie et al., 2018; Jiang et al., 2019; Thomi et al., 2019). Therefore, the exosomes used in the present study were isolated from HUCMSCs. To optimize the concentration of exosomes for use with OECs, CCK-8 assays were performed to analyze cell viability. When the exosome concentration was 400 μg/mL, CCK-8 values at 12, 24, and 48 hours were significantly higher than with other exosome concentrations. In addition, EdU-labeling indicated significantly higher proliferation of OECs with 400 μg/mL exosomes compared with lower concentrations. The exosome concentration used in the present experiment was consistent with that in previous studies (Sun et al., 2018;

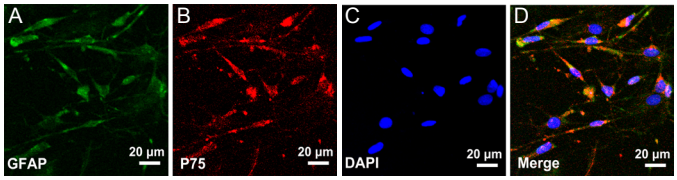

Figure 1 Characterization of OECs.
(A, B) The expression of GFAP and p75 in OECs, respectively. (C) DAPI nuclear counterstaining. (D) Merged figure of A–C. Cells were more than 96% OECs. DAPI: 4′,6-Diamidino-2-phenylindole; GFAP: glial fibrillary acidic protein; OECs: olfactory enshealting cells.

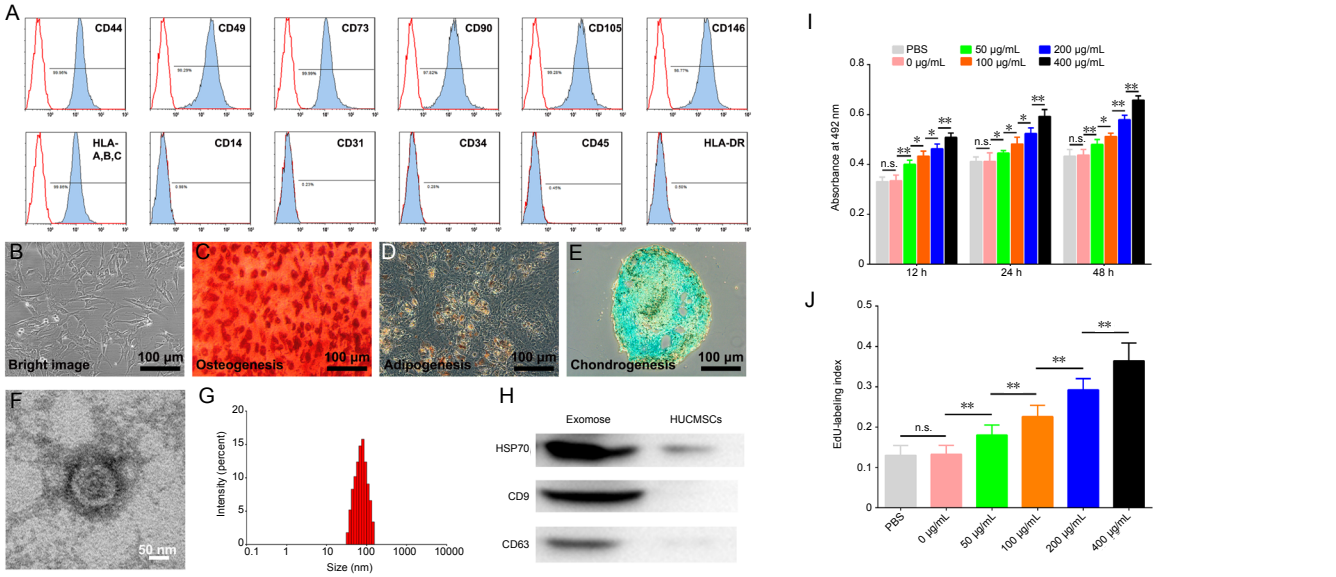

Figure 2 Effect of HUCMSC-derived exosomes on OECs.
(A) Surface markers of HUCMSCs were analyzed by flow cytometry. (B) Representative image of HUCMSCs detected by light microscopy. (C–E) Representative images of osteocyte differentiation (C), adipocyte differentiation (D), and chondrocyte differentiation (E) of HUCMSCs. Arrowheads indicate the characteristic morphology. (F) Transmission electron microscopy image of a HUCMSC exosome. (G) Particle distribution of HUCMSC exosomes was evaluated using a Zetasizer Nano ZS. (H) HUCMSC exosomes were analyzed by western blotting. Quantification of HSP70, CD9, and CD63 is shown in Additional Figure 1. (I) Cell Counting Kit 8 values of viable OECs (n = 5 for each group). (J) EdU-labeling index of OECs (n = 10 for each group). All data represent the mean ± SEM. *P < 0.05, **P < 0.01 (one-way analysis of variance followed by Bonferroni's test). EdU: 5-Ethynyl-2′-deoxyuridine; HSP70: heat shock protein 70; HUCMSCs: human umbilical cord mesenchymal stem cells; n.s.: not significant; OECs: olfactory enshealting cells.

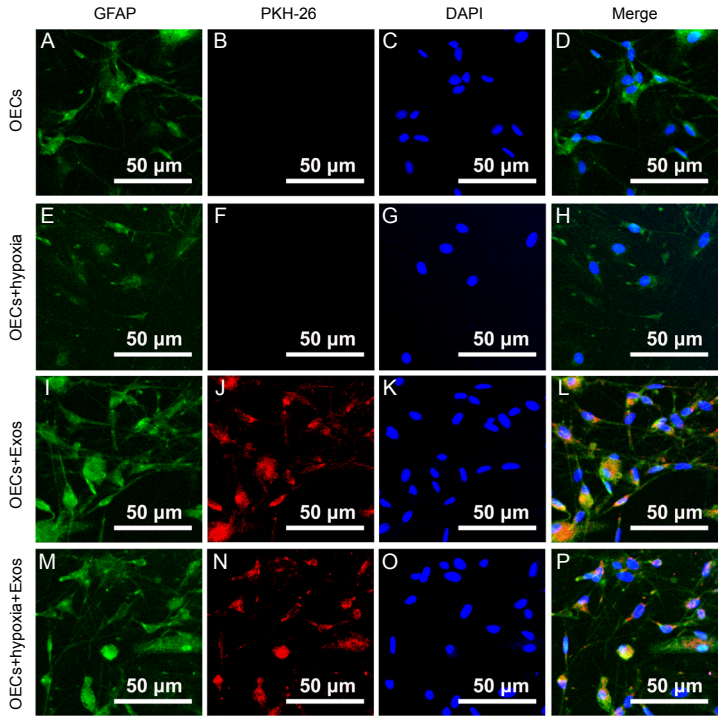

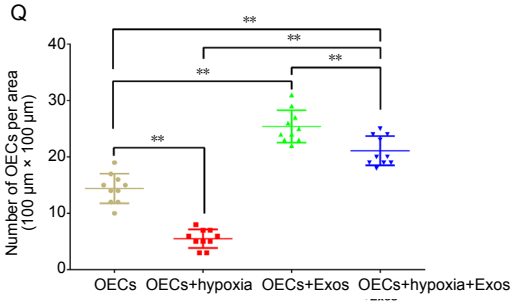

Figure 3 The effect of HUCMSC exosomes on OECs under hypoxic conditions for 24 hours.
(A–D) Representative images of OECs in normal conditions. (E–H) Representative images of OECs under hypoxic conditions. The number of OECs in the OECs + hypoxia group was the least among the groups. (I–L) Representative images of OECs and exosomes in normal conditions. The number of OECs in the OECs + Exos group was more than that in other groups. (M–P) Representative images of OECs and exosomes under hypoxic conditions. The number of OECs in the OECs + hypoxia + Exos group was more than that in the OECs + hypoxia group. (Q) Quantification of OECs in each group (n = 10 for each group). All data represent the mean ± SEM. **P < 0.01 (one-way analysis of variance followed by Bonferroni's test). Exos: Exosomes; HUCMSCs: human umbilical cord mesenchymal stem cells; OECs: olfactory enshealting cells.

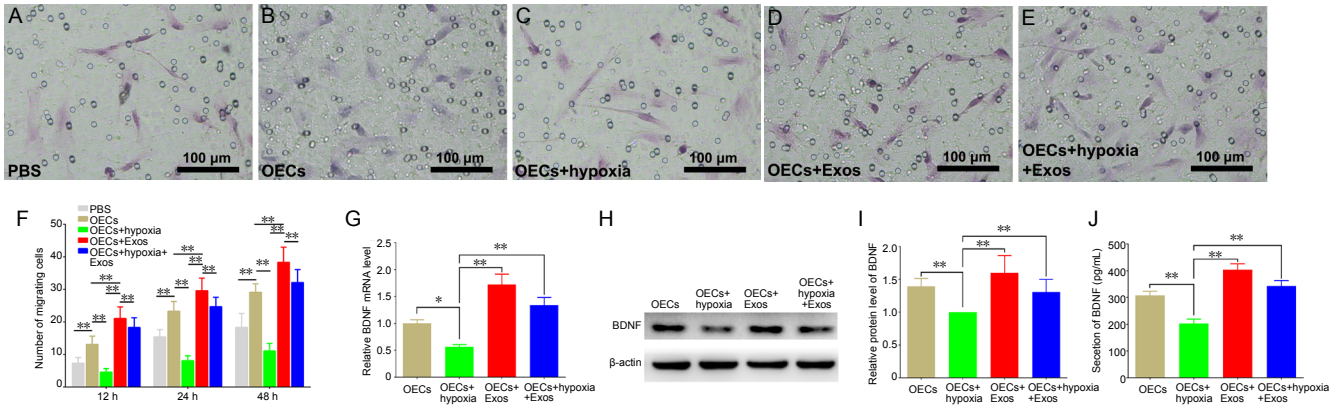

Figure 4 Effect of HUCMSC exosomes on the migration of OECs under hypoxic conditions.
(A–E) Transwell experiment. (A) Representative photos of migrating OECs in the PBS group at 24 hours. The number of migrating OECs in the PBS group was 15.4 ± 2.22. (B) Representative photos of migrating OECs in normal conditions at 24 hours. The number of migrating OECs in the OECs group was 23.3 ± 3.02. (C) Representative photos of migrating OECs under hypoxic conditions at 24 hours. The number of migrating OECs in the OECs group was 8.1 ± 1.52, which was the least among the five groups. (D) Representative photos of migrating OECs in the exosomes group at 24 hours. The number of migrating OECs in the OECs group was 29.6 ± 3.86, which was more than other groups. (E) Representative photos of migrating OECs under hypoxic conditions in the exosomes group at 24 hours. The number of migrating OECs in the OECs group was 24.7 ± 2.87, which was similar to that in the OECs group. (F) The quantification of migrating OECs in each group (n = 10 for each group). (G) Relative Bdnf mRNA level detected by qRT-PCR (n = 3 for each group). (H) Western blotting of BDNF in each group (n = 3 for each group). (I) Relative protein level of BDNF in each group (n = 3 for each group). (J) Secretion level of BDNF detected by ELISA (n = 10 for each group). All data represent the mean ± standard error of the mean. $*P < 0.05$, $**P < 0.01$ (one-way analysis of variance followed by Bonferroni's test). BDNF: Brain-derived neurotrophic factor; ELISA: enzyme linked immunosorbent assay; Exos: exosomes; HUCMSCs: human umbilical cord mesenchymal stem cells; OECs: olfactory enshealting cells; qRT-PCR: quantitative real-time polymerase chain reaction.

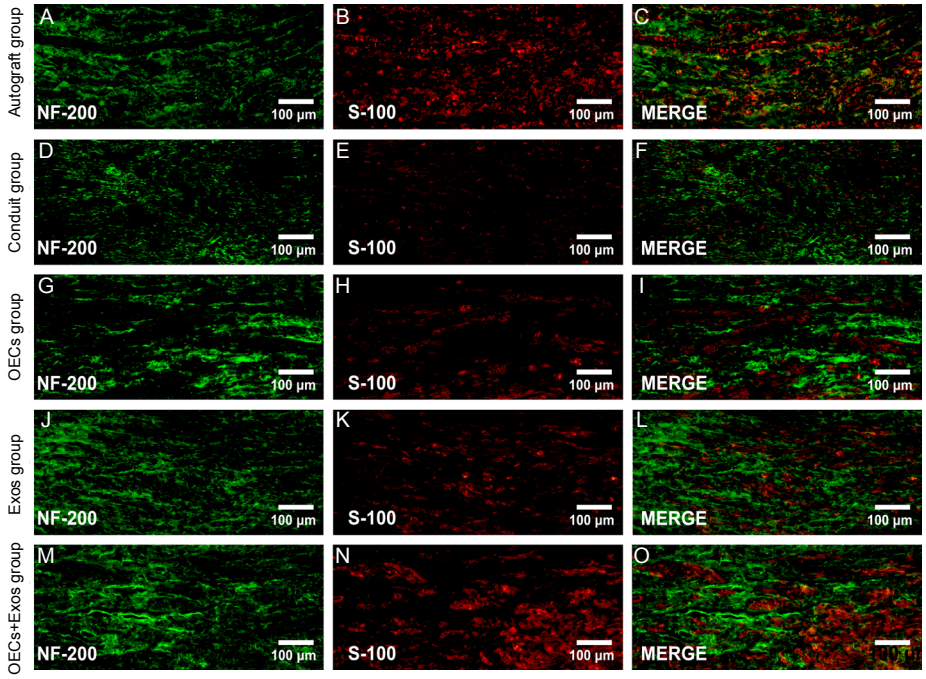

Figure 5 Effect of OECs and exosomes on sciatic nerve regeneration at 12 weeks post-surgery (double immuofluorescence staining).
(A–C) Representative photos of regenerated nerves in the autograft group. (D–F) Representative photos of regenerated nerves in the conduits group. (G–I) Representative photos of regenerated nerves in the OECs group. (J–L) Representative photos of regenerated nerves in the Exos group. (M–O) Representative photos of regenerated nerves in the OECs + Exos group. All images show that the OECs + Exos group and the Autograft group had similar regenerated nerve fibers, which were more than those in the OECs and Exos groups; however, the conduit group showed the smallest number of regenerated fibers. Exos: Exosomes; N-200: neurofilament 200; OECs: olfactory enshealting cells.

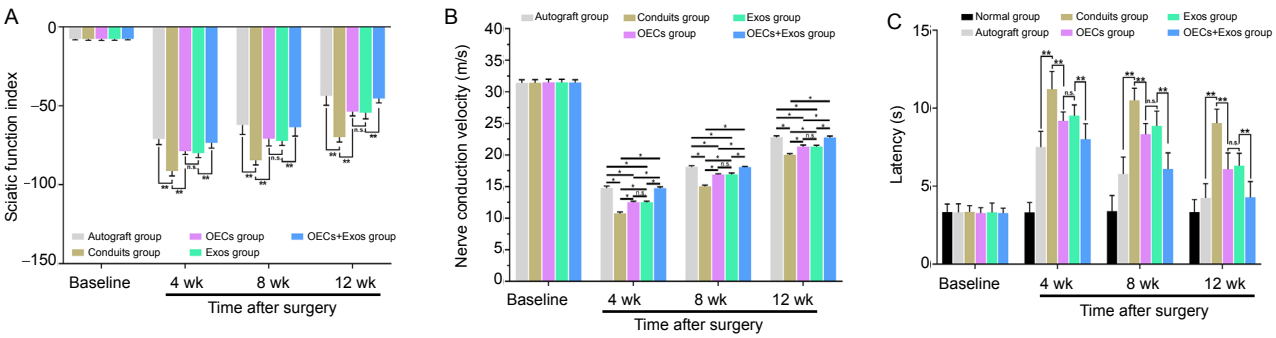

Figure 6 Synergistic effect of OECs and exosomes on the functional recovery of sciatic nerve injury rats.
(A) Sciatic funtional index (n = 10). (B) Nerve conduction velocity values in each group (n = 6). (C) Hind paw nerve conduction latency in electrophysiological evaluation (n = 6). The data represent the mean ± standard error of the mean. $*P < 0.05$, $**P < 0.01$, *vs.* Exos group (one-way analysis of variance followed by Bonferroni's test). Exos: Exosomes; n.s., not significant; OECs: olfactory enshealting cells.

Jiang et al., 2019), indicating 400 μg/mL to be the optimal concentration.

We then analyzed exosome distribution and cell numbers under hypoxic conditions by immunofluorescence labeling. We found that the number of GFAP- and DAPI-stained OECs was significantly increased in the OECs + Exos group compared with that in the OECs group, indicating that exosomes were capable of enhancing the number of OECs in normal conditions. When OECs were exposed to a hypoxic environment, the number of fluorescence-labeled cells was significantly decreased, indicating that hypoxia was deleterious to OECs. Moreover, PKH26-labeled exosomes were cytoplasmically distributed in OECs under hypoxic conditions, and the number of OECs was significantly enhanced compared with that in the OECs + hypoxia group. However, exosomes had a partial effect on OEC survival in hypoxic conditions, because the number of OECs in the OECs + Exos group was higher than that in the OECs + hypoxia + Exos group. Together, these findings demonstrate that exosomes can promote the survival of OECs under hypoxic conditions.

We then investigated the migratory capability of OECs using Transwell chamber assays. Significantly increased numbers of migrated OECs were observed with exosomes in normal conditions, indicating that exosomes promoted the migration of OECs. In addition, the number of migrated OECs in hypoxic conditions were significantly decreased. Interestingly, exosomes were able to enhance the number of migrated OECs under hypoxic conditions, indicating that exosomes from HUCMSCs can promote the intrinsic migratory ability of OECs, especially in hypoxic conditions.

Next, we evaluated the mechanism by which the *in vitro* migratory effect of OECs is enhanced. BDNF is a secreted neurotrophic factor that is crucial for development of the mammalian nervous system and that promotes survival of motor neurons following nerve injury (Liu et al., 2014; Wang et al., 2016). BDNF can promote the migration of OECs through transient receptor potential cation channels (Wang et al., 2016). Moreover, HUCMSC exosomes can enhance the migration ability of several types of cells, such as skin dermal fibroblasts (Bakhtyar et al., 2018), human umbilical vein endothelial cells (Zhang et al., 2015), and cardiac fibroblasts (Zhao et al., 2015) via various signaling pathways. In the present experiment, exosome administration increased the gene expression, protein level and secretion of BDNF in OECs under hypoxic conditions, indicating that exosomes might trigger the inherent mechanism that activates BDNF signaling to improve the migratory capability of OECs in hypoxia.

Although the mechanism by which exosomes promote BDNF expression and secretion from OECs under hypoxic conditions is unclear, a few possibilities can be discussed. Exosomes from HUCMSCs can undertake functions via microRNAs. Exosome-mediated transfer of microRNAs had been reported to improve therapeutic efficacy in sepsis (Song et al., 2017), promote the cell cycle and inhibit apoptosis (Zhu et al., 2019b), and attenuate burn-induced inflammation (Li et al., 2016). Therefore, it is possible that HUCMSCs release exosomal microRNAs, which cross the OEC membrane to promote BDNF signaling and improve OEC migration in hypoxic conditions. Further studies are needed to confirm the intrinsic mechanism that is crucial for the therapeutic effect of exosomes.

To analyze the combined effect of OECs and exosomes on peripheral nerve repair, a 12 mm sciatic nerve defect model was used, which models a severe peripheral nerve injury (Wang et al., 2013). Double NF-200/S-100 immunofluorescence staining of regenerated nerves revealed that OECs combined with exosomes had more evenly distributed regenerating axons and migrated Schwann cells compared with OEC or exosome treatment alone, indicating that exosomes might enhance the survival and migration of OECs *in vivo* to create a tunable micro-milieu for the regeneration of the severed axons (Deumens et al., 2006). The combination of OECs and exosomes was able to improve the SFI and nerve conduction velocity for functional motor recovery and the latency time of hind paw withdrawal for sensory functional recovery, suggesting that more regenerated nerve fibers might successfully migrate through the conduits from the proximal to the distal end because of the neurotrophic function of OECs and exosomes (Liu et al., 2018; Shiue et al., 2019).

Although the intrinsic mechanism underlying the enhanced regenerative performance of Schwann cells and axons was not clear, several possibilities can be discussed. Previous studies have reported that endogenous Schwann cells are the main facilitators of the peripheral nervous system and when a nerve injury, such as nerve transection, occurs, they retract from damaged axons and subsequently show low expression levels of several molecules, including nerve growth factor, BDNF, and p75 nerve growth factor receptor, which are crucial for axonal regeneration (Radtke and Kocsis, 2012). However, Wright et al. (2018) demonstrated that transplanted OECs were capable of expressing these factors following transplantation. Moreover, cut axons exert a 'die-back' phenomenon, which is retraction from the original site by several millimeters. Transplanted OECs can instantly provide neurotrophic factors for the regenerating axons to reduce the 'die-back' and to direct the proximal nerve stump for improved regeneration (Radtke and Kocsis, 2012; Kabiri et al., 2015). In addition, Shiue et al. (2019) reported that HUCMSC exosomes can prevent neuroinflammation and enhance the level of anti-inflammatory cytokines (such as interleukin 10) and neurotrophic factors (such as BDNF and glial cell line-derived neurotrophic factor), which is beneficial for nerve regeneration. Therefore, the combination of OECs and HUCMSC exosomes can synergistically improve the micro-environment, support the survival of Schwann cells and axons, and promote sciatic nerve regeneration.

Taken together, our results indicate that HUCMSC exosomes (400 μg/mL) can improve the viability and migration of OECs in hypoxic conditions by activating BDNF signaling. The synergism of OECs and exosomes promoted nerve regeneration and functional recovery. This study highlights a potential therapeutic strategy using OECs for severe nerve injury, which often has to overcome a hypoxic environment.

Acknowledgments: *We thank the Mr. Jin-Tao Hu (Department of Immunology, Air Force Medical University, China), Mr. Hai-Feng Zhang (Department of Neurobiology, Air Force Medical University, China), and Mr. Xi-Wang Hu (Third Affiliated Hospital, Air Force Medical University, China) for providing excellent technical assistance.*

Author contributions: *Study conception and design: YZ, WTW, CL, MS; data analysis and interpretation: YZ, CL, MS; manuscript drafting:*

YZ, WTW, CRG, CL, MS; manuscript revising: CL, MS. All authors approved the final version of the paper.

Conflicts of interest: *The authors declare that they have no competing interests.*

Financial support: *This work was supported by grants from the National Natural Science Foundation of China, No.81872699 (to MS), Key project of Shaanxi Province, China, No. 2017ZDXM-SF-043 (to MS), and the Military Medical Science and Technology Youth Development Program, China, No. 19QNP061 (to CL). The funding sources had no role in study conception and design, data analysis or interpretation, paper writing or deciding to submit this paper for publication.*

Institutional review board statement: *The study was approved by the Institutional Ethical Committee of the Air Force Medical University, China (approval No. IACUC-20181004) on October 7, 2018. Human umbilical cords were collected from two full-term pregnant women after cesarean delivery with the prior written informed consent signed by the women and the approval authorized by the Ethics Committee of the Linyi People's Hospital, China (approval No. 30054) on May 20, 2019.*

Declaration of patient consent: *The authors certify that they have obtained the consent forms from both pregnant women. In the forms, they have given their consent for their images and other clinical information to be reported in the journal. The women understood that their names and initials would not be published and due efforts will be made to conceal their identity.*

Data sharing statement: *Datasets analyzed during the current study are available from the corresponding author on reasonable request.*

Plagiarism check: *Checked twice by iThenticate.*

Peer review: *Externally peer reviewed.*

References

Bakhtyar N, Jeschke MG, Herer E, Sheikholeslam M, Amini-Nik S (2018) Exosomes from acellular Wharton's jelly of the human umbilical cord promotes skin wound healing. Stem Cell Res Ther 9:193.

Beecher K, St John JA, Chehrehasa F (2018) Factors that modulate olfactory dysfunction. Neural Regen Res 13:1151-1155.

Carvalho LA, Teng J, Fleming RL, Tabet EI, Zinter M, de Melo Reis RA, Tannous BA (2019) Olfactory ensheathing cells: a trojan horse for glioma gene therapy. J Natl Cancer Inst 111:283-291.

de Farias CB, Heinen TE, dos Santos RP, Abujamra AL, Schwartsmann G, Roesler R (2012) BDNF/TrkB signaling protects HT-29 human colon cancer cells from EGFR inhibition. Biochem Biophys Res Commun 425:328-332.

Deumens R, Koopmans GC, Honig WMM, Hamers FPT, Maquet V, Jérôme R, Steinbusch HWM, Joosten EAJ (2006) Olfactory ensheathing cells, olfactory nerve fibroblasts and biomatrices to promote long-distance axon regrowth and functional recovery in the dorsally hemisected adult rat spinal cord. Exp Neurol 200:89-103.

Gomes ED, Mendes SS, Assunção-Silva RC, Teixeira FG, Pires AO, Anjo SI, Manadas B, Leite-Almeida H, Gimble JM, Sousa N, Lepore AC, Silva NA, Salgado AJ (2018) Co-transplantation of adipose tissue-derived stromal cells and olfactory ensheathing cells for spinal cord injury repair. Stem Cells 36:696-708.

Gu J, Xu H, Xu YP, Liu HH, Lang JT, Chen XP, Xu WH, Deng Y, Fan JP (2019) Olfactory ensheathing cells promote nerve regeneration and functional recovery after facial nerve defects. Neural Regen Res 14:124-131.

Hare GM, Evans PJ, Mackinnon SE, Best TJ, Bain JR, Szalai JP, Hunter DA (1992) Walking track analysis: a long-term assessment of peripheral nerve recovery. Plast Reconstr Surg 89:251-258.

Jiang L, Zhang S, Hu H, Yang J, Wang X, Ma Y, Jiang J, Wang J, Zhong L, Chen M, Wang H, Hou Y, Zhu R, Zhang Q (2019) Exosomes derived from human umbilical cord mesenchymal stem cells alleviate acute liver failure by reducing the activity of the NLRP3 inflammasome in macrophages. Biochem Biophys Res Commun 508:735-741.

Kabiri M, Oraee-Yazdani S, Shafiee A, Hanaee-Ahvaz H, Dodel M, Vaseei M, Soleimani M (2015) Neuroregenerative effects of olfactory ensheathing cells transplanted in a multi-layered conductive nanofibrous conduit in peripheral nerve repair in rats. J Biomed Sci 22:35.

Li X, Liu L, Yang J, Yu Y, Chai J, Wang L, Ma L, Yin H (2016) Exosome derived from human umbilical cord mesenchymal stem cell mediates miR-181c attenuating burn-induced excessive inflammation. EBioMedicine 8:72-82.

Liu Q, Qin Q, Sun H, Zhong D, An R, Tian Y, Chen H, Jin J, Wang H, Li G (2018) Neuroprotective effect of olfactory ensheathing cells co-transfected with Nurr1 and Ngn2 in both in vitro and in vivo models of Parkinson's disease. Life Sci 194:168-176.

Liu Z, Huang L, Liu L, Luo B, Liang M, Sun Z, Zhu S, Quan X, Yang Y, Ma T, Huang J, Luo Z (2014) Activation of Schwann cells in vitro by magnetic nanocomposites via applied magnetic field. Int J Nanomedicine 10:43-61.

Montagne-Clavel J, Oliveras JL (1996) The "plantar test" apparatus (Ugo Basile Biological Apparatus), a controlled infrared noxious radiant heat stimulus for precise withdrawal latency measurement in the rat, as a tool for humans? Somatosens Motor Res 13:215-223.

Nie W, Ma X, Yang C, Chen Z, Rong P, Wu M, Jiang J, Tan M, Yi S, Wang W (2018) Human mesenchymal-stem-cells-derived exosomes are important in enhancing porcine islet resistance to hypoxia. Xenotransplantation 25:e12405.

Radtke C, Kocsis JD (2012) Peripheral nerve injuries and transplantation of olfactory ensheathing cells for axonal regeneration and remyelination: fact or fiction? Int J Mol Sci 13:12911-12924.

Riggio C, Nocentini S, Catalayud MP, Goya GF, Cuschieri A, Raffa V, del Río JA (2013) Generation of magnetized olfactory ensheathing cells for regenerative studies in the central and peripheral nervous tissue. Int J Mol Sci 14:10852-10868.

Shi W, Huang CJ, Xu XD, Jin GH, Huang RQ, Huang JF, Chen YN, Ju SQ, Wang Y, Shi YW, Qin JB, Zhang YQ, Liu QQ, Wang XB, Zhang XH, Chen J (2016) Transplantation of RADA16-BDNF peptide scaffold with human umbilical cord mesenchymal stem cells forced with CXCR4 and activated astrocytes for repair of traumatic brain injury. Acta Biomater 45:247-261.

Shiue SJ, Rau RH, Shiue HS, Hung YW, Li ZX, Yang KD, Cheng JK (2019) Mesenchymal stem cell exosomes as a cell-free therapy for nerve injury-induced pain in rats. Pain 160:210-223.

Song Y, Dou H, Li X, Zhao X, Li Y, Liu D, Ji J, Liu F, Ding L, Ni Y, Hou Y (2017) Exosomal miR-146a contributes to the enhanced therapeutic efficacy of interleukin-1β-primed mesenchymal stem cells against sepsis. Stem Cells 35:1208-1221.

Sun Y, Shi H, Yin S, Ji C, Zhang X, Zhang B, Wu P, Shi Y, Mao F, Yan Y, Xu W, Qian H (2018) Human mesenchymal stem cell derived exosomes alleviate type 2 diabetes mellitus by reversing peripheral insulin resistance and relieving β-cell destruction. ACS Nano 12:7613-7628.

Suzuki Y, Tanihara M, Ohnishi K, Suzuki K, Endo K, Nishimura Y (1999) Cat peripheral nerve regeneration across 50 mm gap repaired with a novel nerve guide composed of freeze-dried alginate gel. Neurosci Lett 259:75-78.

Thomi G, Surbek D, Haesler V, Joerger-Messerli M, Schoeberlein A (2019) Exosomes derived from umbilical cord mesenchymal stem cells reduce microglia-mediated neuroinflammation in perinatal brain injury. Stem Cell Res Ther 10:105.

Wang B, Li P, Shangguan L, Ma J, Mao K, Zhang Q, Wang Y, Liu Z, Mao K (2018) A novel bacterial cellulose membrane immobilized with human umbilical cord mesenchymal stem cells-derived exosome prevents epidural fibrosis. Int J Nanomedicine 13:5257-5273.

Wang Y, Teng HL, Gao Y, Zhang F, Ding YQ, Huang ZH (2016) Brain-derived neurotrophic factor promotes the migration of olfactory ensheathing cells through TRPC channels. Glia 64:2154-2165.

Wang Y, Qi F, Zhu S, Ye Z, Ma T, Hu X, Huang J, Luo Z (2013) A synthetic oxygen carrier in fibrin matrices promotes sciatic nerve regeneration in rats. Acta Biomater 9:7248-7263.

Wright AA, Todorovic M, Tello-Velasquez J, Rayfield AJ, St John JA, Ekberg JA (2018) Enhancing the Therapeutic Potential of Olfactory Ensheathing Cells in Spinal Cord Repair Using Neurotrophins. Cell Transplant 27:867-878.

Xu H, Wang Z, Liu L, Zhang B, Li B (2020) Exosomes derived from adipose tissue, bone marrow, and umbilical cord blood for cardioprotection after myocardial infarction. J Cell Biochem 121:2089-2102.

Zhang B, Wu X, Zhang X, Sun Y, Yan Y, Shi H, Zhu Y, Wu L, Pan Z, Zhu W, Qian H, Xu W (2015) Human umbilical cord mesenchymal stem cell exosomes enhance angiogenesis through the Wnt4/β-catenin pathway. Stem Cells Transl Med 4:513-522.

Zhang C, Yin X, Zhang J, Ao Q, Gu Y, Liu Y (2017) Clinical observation of umbilical cord mesenchymal stem cell treatment of severe idiopathic pulmonary fibrosis: A case report. Exp Ther Med 13:1922-1926.

Zhang L, Li B, Liu B, Dong Z (2019a) Co-transplantation of epidermal neural crest stem cells and olfactory ensheathing cells repairs sciatic nerve defects in rats. Front Cell Neurosci 13:253.

Zhang ZG, Buller B, Chopp M (2019b) Exosomes - beyond stem cells for restorative therapy in stroke and neurological injury. Nat Rev Neurol 15:193-203.

Zhao P, Qiao J, Huang S, Zhang Y, Liu S, Yan LY, Hsueh AJW, Duan EK (2011) Gonadotrophin-induced paracrine regulation of human oocyte maturation by BDNF and GDNF secreted by granulosa cells. Hum Reprod 26:695-702.

Zhao Y, Sun X, Cao W, Ma J, Sun L, Qian H, Zhu W, Xu W (2015) Exosomes derived from human umbilical cord mesenchymal stem cells relieve acute myocardial ischemic injury. Stem Cells Int 2015:761643.

Zhu S, Ge J, Wang Y, Qi F, Ma T, Wang M, Yang Y, Liu Z, Huang J, Luo Z (2014) A synthetic oxygen carrier-olfactory ensheathing cell composition system for the promotion of sciatic nerve regeneration. Biomaterials 35:1450-1461.

Zhu Y, Zhang Q, Shi X, Han D (2019a) Hierarchical hydrogel composite interfaces with robust mechanical properties for biomedical applications. Adv Mater 31:e1804950.

Zhu Z, Zhang Y, Zhang Y, Zhang H, Liu W, Zhang N, Zhang X, Zhou G, Wu L, Hua K, Ding J (2019b) Exosomes derived from human umbilical cord mesenchymal stem cells accelerate growth of VK2 vaginal epithelial cells through MicroRNAs in vitro. Hum Reprod 34:248-260.

C-Editor: Zhao M; S-Editors: Yu J, Li CH; L-Editors: Yu J, Song LP; T-Editor: Jia Y